THE JOURNAL OF PHYSICAL CHEMISTRY C

Article

Study of the Nature and Location of Silver in Ag-exchanged Mordenite Catalysts. Characterization by Spectroscopic Techniques

Soledad Guadalupe Aspromonte, Martin D. Mizrahi, Florencia A. Schneeberger, José Martín Ramallo López, and Alicia V. Boix

J. Phys. Chem. C, **Just Accepted Manuscript** • Publication Date (Web): 18 Nov 2013

Study of the Nature and Location of Silver in Ag-exchanged Mordenite Catalysts. Characterization by Spectroscopic Techniques

Soledad G. Aspromonte[a,*], Martín D. Mizrahi[b], Florencia A. Schneeberger[a], José M. Ramallo López[b], Alicia V. Boix[a]

[a] Instituto de Investigaciones en Catálisis y Petroquímica – INCAPE (FIQ, UNL-CONICET) - Santiago del Estero 2829, 3000, Santa Fe, Argentina.

[b] Instituto de Investigaciones Fisicoquímicas Teóricas y Aplicadas – INIFTA (CCT La Plata – CONICET, UNLP) – Diagonal 113 y calle 64, 1900, La Plata, Argentina.

Corresponding author. Tel: +54 03424536861
[*]E-mail address: saspromonte@fiq.unl.edu.ar

Submitted to the Journal of Physical Chemistry C

Abstract

Catalysts based on Na-mordenite (symbolized as 'M') exchanged with 5, 10 and 15 wt. % of Ag were characterized by XPS, EXAFS, XANES and UV-Vis DRS spectroscopic techniques in order to investigate the effect of different treatments on the chemical state and surface concentration of silver species. The Ag_xM catalysts were analyzed in oxidizing (O_2) or reducing (H_2/Ar) atmospheres and also after being used in the selective catalytic reduction of NOx or in successive cycles of toluene adsorption/desorption.

In calcined samples, EXAFS profiles showed two types of Ag-O spheres of coordination, one due to a dispersed phase of silver oxide and the other, to Ag^+ ions in interaction with the oxygen of the zeolite framework. The UV-Vis DRS spectra showed the coexistence of isolated Ag^+, $Ag_n^{\delta+}$ ($n < 10$) cationic clusters and Ag_xO particles. In addition, through the modified Auger parameter (α'), calculated from XPS measurements, it was possible to identify Ag^+ ions at exchange sites (α'~722 eV) and Ag_xO (α'~725 eV) highly dispersed on the surface. Both species constitute stable active centers for the SCR of NOx under severe reaction conditions. However, during the adsorption-desorption of toluene, the reduction of silver oxides produces Ag(0) due to thermal hydrocarbon decomposition.

Keywords: silver-exchanged mordenite; EXAFS-XANES; XPS; UV-Vis DRS; Auger parameter.

Introduction

Materials based on silver species have attracted considerable interest because of their potential applications in areas such as catalysis, nano-electronics and optical filters.[1-8] Particularly, silver-based catalysts have become the object of several studies for the abatement of nitrogen oxides (NOx) and unburnt hydrocarbon (HCs) emissions from exhaust gas streams. Ag/Al_2O_3 is known to be one of the most effective catalysts for the selective catalytic reduction of NOx (SCR-NOx) with hydrocarbons.[9-17] Silver-zeolite catalysts present similar characteristics but, in addition, they have unique ion-exchanged properties. Microporous solids are of scientific and technological interest because of their ability to interact with atoms, ions and molecules not only at their outer surfaces, but also throughout the inner porous network. In the same way, the presence of charge compensation cations within the porosity of the inorganic framework gives the ability of ionic exchange to the zeolites, allowing the incorporation of different metals to generate catalytic properties widely applied in industry. To better understand issues as varied as the mechanism of selective reduction of NOx or the hydrocarbon adsorption process of silver based catalysts, it is necessary to determine the chemical state and the location of silver nanoparticles in the zeolitic framework.[3, 13, 18, 19]

Recently, a considerable number of studies have explored the catalytic properties of silver-zeolite catalysts for the SCR of NOx by hydrocarbons[20-22] or alcohols.[23-25] Our research group reported that silver-exchanged Na-mordenite catalysts were active and selective in the removal of nitrogen oxides using butane or toluene as reducing agents.[26] In the same way, these materials were able to trap hydrocarbons like toluene at low temperature and to retain them up to 250 °C.[27] From this temperature, the adsorbed hydrocarbons and NOx can react. Different types of silver species are present in these

catalysts, depending on the preparation and pretreatment conditions as well as on the nature of the process in which the catalysts were used.

Accordingly, this work was undertaken with the aim of identifying the chemical state of silver species in Na-mordenite, which were prepared by the ion-exchange method and treated under different gaseous environments. In addition, the present study also analyzed the changes caused by the use of the prepared samples as catalysts in the reaction of selective catalytic reduction of NOx with butane, or as adsorbent of toluene, after successive cycles of adsorption-desorption.

X-ray absorption near edge spectroscopy (XANES) was used to determine the local structure and electronic characteristics of the Ag species confined in the microporous network of Na-mordenite. In addition, some structural properties of the silver species anchored in the support were determined by extended x-ray absorption fine structure (EXAFS). In addition, UV-Vis diffuse reflectance spectroscopy (UV-Vis DRS), which provides a sensitive measure of the chemical state of materials, and X-ray photoelectron spectroscopy (XPS) were used to determine the oxidation state and surface concentration of silver species. This approach provides valuable insights into the catalytic properties exhibited by the active catalyst and the behavior of the AgNa-mordenite sample as hydrocarbon adsorbents.

Experimental Section

Materials preparation

The method employed to prepare silver-exchanged zeolite Na-mordenite consisted in adding 150 ml of aqueous silver (I) nitrate solution (0.04-0.10 M) to exchange 4 g of commercial zeolite NaMOR (Zeolyst International, $Na_{6.4}(AlO_2)_{6.4}(SiO_2)_{41.6}$) at room temperature. The mixture was stirred for 24 h in order to exchange Na^+ by Ag^+ ions.

Then, the samples were filtered and carefully washed with deionized water. All the above steps were performed in a dark room to avoid contact with light which could result in the partial reduction of the Ag^+ species. The resulting solids were dried overnight at 120 °C and then calcined in O_2 flow at a heating rate of 5 °C·min^{-1} to 500 °C and then, the temperature was kept constant for 2 hours.

The exchange degrees were determined on the basis of concentration of cations (Na^+ and Ag^+) in the solid, measured by Flame Atomic Absorption Spectrometry (FAAS). The exchange degree was determined considering that each monovalent Na^+ ion was exchanged with one monovalent Ag^+ ion. Hereafter, the catalyst will be designated as Ag_xM, where 'x' represents the silver content (wt. %). Samples with 5, 10 and 15 wt. % Ag were obtained and the exchange degree was 23.8, 46.9 and 73.4 %, respectively.

Besides, a mechanical mixture between Ag_2O and NaMOR (Ag_2O/M) was prepared to obtain a solid with 15 wt. % Ag and it was used as reference sample.

XPS measurements

The surface chemical composition of the samples was studied by XPS in an ultrahigh vacuum (UHV). For the XPS, the catalysts powders (50 mg) were pressed into pellets with a diameter of ca. 13 mm. Prior to the measurements, all the samples were evacuated in the pretreatment chamber at a pressure lower than 10^{-7} kPa, heating slowly from room temperature to 300 °C. The temperature was kept constant during 30 minutes, in order to remove water and other adsorbed species.

The XPS measurements were carried out using a multitechnique system (SPECS) equipped with a dual Mg/Al X-ray source and a hemispherical PHOIBOS 150 analyzer operating in the fixed analyzer transmission (FAT) mode. The spectra were obtained with a pass energy of 30 eV using Mg Kα X-ray source (hν = 1253.6 eV) operated at

200 W and 12 kV. The working pressure in the analyzing chamber was less than 5 x 10^{-10} kPa.

The binding energy (BE) of core-levels O 1s, Si 2p, Al 2p, C 1s, Na 1s and Ag 3d was measured. Because the C 1s line is highly sensitive to different treatments, the Si 2p peak at 102.3 ± 0.1 eV binding energy was taken as an internal reference.

The binding energy positions of Ag 3d were not enough to identify the oxidation state of the silver species because the characteristic states of oxidized (Ag_2O) and metallic silver are close together (within 0.5 eV).[6] Thus, the kinetic energy (KE) in the Ag MNN region of the Auger transitions was measured and the modified Auger parameter (α') was used to characterize the chemical state of silver. This parameter is the sum of the kinetic energy of the Auger electron (Ag $M_4N_{4,5}N_{4,5}$) and the binding energy of the core-level (Ag $3d_{5/2}$) peak.[28] This parameter was independent of the charging, but still sensitive to the chemical state of silver and it was calculated according to Eq. 1:

$$\alpha' \text{ (eV)} = KE \text{ (Ag } M_4N_{4,5}N_{4,5}) - KE \text{ (Ag } 3d_{5/2}) + h\nu \qquad \text{Eq. 1}$$

where KE (Ag $M_4N_{4,5}N_{4,5}$) is the kinetic energy of the Auger transition, KE (Ag $3d_{5/2}$) is the kinetic energy of the Ag $3d_{5/2}$ core-level and hν is the photon energy equal to 1253.6 eV.

The data treatment was performed with the Casa XPS program (Casa Software Ltd., UK). The peak areas were determined by integration employing a Shirley-type background. Peaks were considered to be a mixture of Gaussian and Lorentzian functions. For the quantification of the elements, sensitivity factors provided by the manufacturer were used.

The XPS analysis of the Ag_xM samples, Ag_2O/M mechanical mixture were performed after different treatments: (a) calcined in O_2 flow at 500 °C (see Materials preparation section) and (b) reduced *in situ* with H_2 (5 %)/Ar flow at 400 ºC for 10 minutes in the reaction chamber of the spectrometer. Ag(0) foil, Ag_2O and $AgNO_3$ provided by Sigma Aldrich were also measured and used as standard samples. For the metallic foil, the spectrum was obtained after using argon ion sputtering. A differentially pumped ion gun was operated at 1 x 10^{-8} kPa, 3 kV and 500 nA, conditions which delivered a sputtering rate of approximately 1 $nm \cdot min^{-1}$. Sputtering was performed in 10 steps of 60 s, followed by 10 steps of 180.

In addition, it is also interesting to know which species are present in the catalytic surface after the catalysts were used in the reaction of the selective catalytic reduction of NOx (SCR-NOx) (treatment c). The reaction was carried out under severe conditions, in a flow reactor fed with a gaseous mixture of (NO + C_4H_{10}) in He with O_2 and 2 % water vapor.[26] In the same vein, the surface of materials was studied after the catalysts were used as adsorbents (treatment d). The adsorption capacities of the Ag_xM samples were evaluated in three cycles of toluene adsorption at 100 °C and desorbed thereof at a programmed-temperature of 500 °C.[27]

EXAFS/XANES

EXAFS experiments at the Ag K edge (25514 eV) were performed using a RIGAKU R-XAS Looper "in-house" spectrometer in transmission mode. Ionization chambers filled with Xe were used to measure the incident radiation and a solid state detector to measure the transmitted intensity. Calcined samples were pressed in pellets with thickness that produced an X-ray absorption jump at the Ag K edge of approximately 0.75. The energy calibration was done using a foil of metallic silver. The quantitative

analysis of the results was performed by modeling and fitting the EXAFS spectra. For this purpose, structures were modeled using the FEFF code[29] and the EXAFS oscillation was isolated and fitted using the ATHENA and ARTEMIS programs, which are graphical interactive software programs for EXAFS analysis based on the IFEFFIT library.[30]

XANES measurements at the Ag L_3 edge were obtained at the SXS beamline at the Laboratorio Nacional de Luz Sincrotron (LNLS) in Campinas (Brazil). Powder samples were pressed on carbon tape. A Si (1 1 1) double-crystal monochromator with a slit aperture of 2.5 mm was used to obtain the desired high resolution of about 0.5 eV. Details of the experimental setup of the SXS beamline have been published elsewhere.[31] The X-ray absorption spectra were recorded in total electron yield (TEY) mode, collecting the emitted current for each photon-energy with an electrometer connected to the sample. Experiments were performed in a vacuum of 10^{-9} kPa at room temperature. The energy scale was calibrated setting the Ag L_3-edge, defined by the first inflection point of the X-ray absorption spectrum of Ag metallic foil sample to 3351 eV. The final TEY XANES spectra were obtained after background subtraction and normalization to the post-edge intensity.

UV-Vis Diffuse reflectance spectroscopy

UV-Visible spectra were recorded at room temperature on a Shimadzu UV-Vis-NIR model UV-3600 spectrometer. Prior to the measurements, all the calcined samples were dried in an oven at 120 °C overnight in order to remove adsorbed water. The spectrometer was equipped with a diffuse-reflectance attachment with an integrating sphere coated by $BaSO_4$, which served as a reference. The absorption intensity was

calculated from the Schuster-Kubelka-Munk equation, $F(R_\infty) = (1-R_\infty)^2 / 2 R_\infty$, where R_∞ is the reflectance.

Results and Discussion

X-ray photoelectron spectroscopy (XPS)

In order to investigate the effect of the different treatments on the chemical state and surface concentration of silver species in the Ag_xM s amples, the photoelectron spectra of samples with different silver contents were analyzed. Prior to the XPS measurement, samples were oxidized with O_2/He flow or reduced *in situ* (H_2/Ar). The samples were also studied after being used as catalysts, on the selective catalytic reduction of NOx or as adsorbents in toluene adsorption.

The Ag 3d core-level and the corresponding X-ray excited Ag MNN Auger spectra obtained for the $Ag_{15}M$ (after different treatments) and for reference compounds are shown in Figure 1. The binding energies (BE) of Ag $3d_{5/2}$ and the modified Auger parameter (α') calculated for Ag_xM, Ag_2O/M (mechanical mixture) and reference compounds are summarized in Table 1.

The Ag 3d region (Fig. 1) shows two peaks corresponding to spin-orbit splitting of Ag $3d_{3/2-5/2}$ with a separation of 6 eV. The Ag $3d_{5/2}$ binding energies measured for calcined samples (treatment a) were 368.5 eV (fwhm = 2.4) for $Ag_{15}M$ and 368.6 eV (fwhm = 2.1) for both $Ag_{10}M$ and Ag_5M catalysts (Table 1), which could belong to Ag^+ ions located at exchange positions or silver oxide particles dispersed in the zeolite channels.

The BE of Ag $3d_{5/2}$ observed for the Ag_xM samples (Table 1) was higher than the values measured for Ag_2O and $AgNO_3$ pure compounds (BE 368.2 eV). Furthermore, the Ag 3d peaks in $Ag_{15}M$ (spectrum a, Fig. 1A), $Ag_{10}M$ (spectrum a, Fig. 2A) and Ag_5M (not shown) were broader than those of pure compounds, which suggests the

presence of more than one species. In addition, it is possible that the binding energy of different silver species (Ag^+ cations and Ag_xO nanoparticles) may be influenced by the zeolite structure (built by tetrahedra of Si, Al and O atoms). For example, the BE of Ag 3d of pure Ag_2O decreased 0.4 eV after being dispersed in the mordenite support by the mechanical mixture (Table 1).

In agreement with our XPS results, Neves and coworkers[19, 32] reported BE values between 368.69 eV and 368.88 eV measured on silver exchanged in different zeolite structures. Also, Anpo and coworkers[33] reported a high BE value (370.5 eV) for the Ag $3d_{5/2}$ core-level in Ag^+/ZSM-5, which was also attributed to silver ions anchored within the structure.

On the other hands, the BE values of the Ag $3d_{5/2}$ peak reported in the literature for different pure compounds are very close, around of 368.1 eV, 367.8 eV and 367.4 eV for Ag(0), Ag_2O and AgO, respectively. [6, 34-36] The relative small shift of the Ag 3d peaks makes it difficult to determine the oxidation state, especially in samples where the silver species are supported in a matrix with high surface area.

In order to overcome this problem, the Ag MNN Auger spectrum was also measured and the modified Auger parameter (α') was calculated. Previous studies have shown that Ag MNN Auger transitions are highly sensitive to the oxidation state of silver.[1, 4, 37] It is reasonable to expect that with varying chemical states, the X-ray excited Ag MNN Auger peaks will exhibit larger energy shifts and shape changes than core-level Ag 3d peaks because a single Auger transition involves three electrons and many-body effects.

The MNN Auger spectra (see Fig. 1B and D) of silver are the combination of two main Auger transitions, namely $M_4N_{45}N_{45}$ and $M_5N_{45}N_{45}$, whose kinetic energy values are around of 358.1 and 349.0 eV, respectively.[38] The shape of the MNN Auger spectrum is complex due to the multiplet splitting of the quasiatomic states superimposed on the

spin-orbit splitting of M_4 and M_5 inner levels.[39] Accordingly, only the α' parameters calculated from signal $M_4N_{45}N_{45}$ will be taken into account in this work. Besides, the spectral region with kinetic energy below 351 eV is mainly due to $M_5N_{45}N_{45}$ Auger transitions.[38]

The Auger spectrum of calcined $Ag_{15}M$ (Fig. 1B, spectrum a) shows a main signal at KE = 353.3 eV and a weak shoulder at 357.2 eV in the $M_4N_{45}N_{45}$ region. Similarly, the kinetic energies of the more intense peaks were 353.5 and 353.2 eV on calcined $Ag_{10}M$ (Fig. 2B, spectrum a) and Ag_5M (not shown), respectively. The spectrum shape of these samples looks somewhat different with respect to the Auger spectra of Ag(I) belonging to $AgNO_3$ and Ag_2O pure compounds (Fig. 1D, spectra a and b). The latter ones present two well-defined regions, with kinetic energies centered at 355.2 and 350.0 eV, corresponding to the $M_4N_{45}N_{45}$ and $M_5N_{45}N_{45}$ levels. Similarly, the Auger spectrum can be observed for the Ag_2O/M mechanical mixture, with kinetic energy peaks at 357.1 and 352.0 eV, respectively.

In this vein, the α' values computed for silver exchanged in mordenite, included in Table 1, resulted 721.8, 722.1 and 721.8 eV for 15, 10 and 5 wt. % Ag, respectively. These values are lower than those calculated for both $AgNO_3$ and Ag_2O (α' = 723.4 eV) which are in agreement with the data reported in the literature.[40] In addition, the weak shoulders at KE of 357.2 eV and 356.4 eV observed in $Ag_{15}M$ and $Ag_{10}M$, respectively (spectrum (a) in Fig. 1B and 2B) could be assigned to Ag_xO small particles. The values of parameter α' are around 725.4 eV and 725.0 eV, respectively, in agreement with the value measured in the Ag_2O/M mechanical mixture (Table 1). Therefore, the main silver species in calcined Ag_xM catalysts would be Ag^+ cations in exchange sites inside the structure.

Effect of reduction with H_2 over silver species

After *in situ* reducing with H_2 flow at 400 °C, $Ag_{15}M$ (Fig. 1A, spectrum b) showed binding energies at 367.6 and 373.6 eV for Ag $3d_{5/2}$ and $3d_{3/2}$ respectively, with a fwhm of 2.0 eV. The pure compounds, Ag_2O and Ag(0) foil (Fig. 1C, spectra c and d), exhibited narrower peaks of Ag 3d, with BE Ag $3d_{5/2}$ = 368.4 eV (Table 1), corresponding to metallic silver, which is in agreement with data reported in the literature.[28, 40]

On the other hand, the Ag M_4NN Auger spectrum of the reduced $Ag_{15}M$ sample (Fig. 1B, spectrum b) presents a distinct peak measured at KE = 358.7 eV, with the α' value of 726.3 eV, assigned to metallic silver. Also, the shape of this spectrum is similar to the profile shown on the metallic silver of the Ag(0) foil, Ag_2O or Ag_2O/M reduced in situ (Fig. 1D).

In the Ag 3d region of reduced $Ag_{10}M$ (Fig. 2A, spectrum b) the peaks presents some asymmetry, likely due to the signal overlapping of different silver species. One of them is more intense and centered at 367.5 eV, with α' = 726.3 eV corresponds to metallic silver. Also, xps data of the reduced Ag_5M catalysts shown Ag(0) species on the sample surface (Table 1).

According to the temperature-programmed reduction (TPR) results reported in our previous work[26], the complete reduction of Ag_2O/M occurs at 200 ºC. However, in $Ag_{15}M$ sample a 44 % of silver is reduced at 222 °C, while the other fraction remains as Ag^+ ions at exchange sites. Similar reduction profiles were observed for lower silver content. The silver species easily reducible were associated to nanoparticles of highly dispersed Ag_2O, and isolated Ag^+ ions sitting inside of main channel in the mordenite. The Ag_2O species are probably formed from the thermal decomposition of AgOH species during the calcinations process. This pathway produces very small particles of

silver oxide which are highly dispersed within cavities, which were not detected by XRD.[27]

Silver species in catalysts after using in SCR reaction

The catalytic performance of the Ag_xM samples demonstrated that these catalysts were active and selective under reaction conditions and that the activity was higher in the presence of oxygen excess and water vapor in the stream.[26] The reaction system is complex due to the fact that a number of parallel and consecutive reactions can take place. The main reaction is the reduction of nitrogen oxides by hydrocarbon, but simultaneously the oxidation and the steam reforming of hydrocarbon could occur. However, the XPS results showed that the catalytic surface did not changed significantly during the reaction. The Ag 3d spectra of the $Ag_{15}M$ and $Ag_{10}M$ catalysts used under SCR conditions (Fig. 1A and Fig. 2A, spectra c) exhibit a binding energy for Ag $3d_{5/2}$ = 368.6 eV (Table 1). The Auger spectrum (c) in Fig. 1B shows a broad peak in the M_4NN region with KE = 352.2 eV and a sharp shoulder at 356.8 eV, with α' values of 720.8 and 725.4 eV, respectively. Like the calcined sample, the first value is associated with Ag^+ exchanged ions and the second one is linked to silver oxides finely dispersed on the zeolitic structure. This first value was 1.0 eV lower than the α' value calculated for the calcined sample, which would indicate that the coordination of silver ions inside the structure has changed during the time on stream. The migration of isolated Ag^+ ions from highly coordinated sites (original sample) to more accessible sites with lower coordination (main channel) and the possible formation of cationic clusters ($Ag_n^{\delta+}$) could be stimulated by the reactant mixture during the chemical reaction.

Silver species on Ag_xM samples after using in toluene adsorption.

The spectrum (d) of Ag 3d (Fig. 1A) of $Ag_{15}M$ and its corresponding Auger signal (Fig. 1B, spectrum d) show no significant change compared with original calcined sample. However, the sample with 10 wt. % Ag, presents a BE shift to 368.1 eV and a broadening of Ag 3d peaks through the toluene adsorption on the silver species (Fig. 2A, spectrum d). In addition, the appearance of a shoulder at KE = 358.4 eV (α' = 726.5 eV) in the Auger region (Fig. 2B, spectrum d) could indicate the presence of metallic silver, which was produced by the reduction of Ag_2O particles. These results suggest that a fraction of silver oxide is reduced in the presence of toluene/He atmosphere. This is in agreement with our previous results, where toluene in contact with silver is decomposed above 400 °C and produces H_2 which reduces the surface of catalyst.[26]

On the other hand, the surface atomic ratio Ag/Al was 1.2 for the calcined $Ag_{15}M$ sample (Table 1), which remained constant during the reaction. However, the dispersion of silver species significantly decreased when the sample was reduced *in situ*. A similar effect was caused by the adsorption-desorption of toluene. Probably, this decrease is linked to the sintering of metal particles under reducing atmosphere and the formation of carbon on the silver particle surface.

Finally, the spectra of the constituent elements of the zeolite structure present a peak in the Al 2p region at 74.1-74.3 eV, with fwhm = 2.2-2.4 eV, and a symmetrical large peak in the O 1s region at 531.8-531.9 eV, with fwhm = 2.4-2.5 eV (not shown). These peaks correspond to the tetrahedral Si or Al atoms, such as SiO_4 or AlO_4 groups, and the oxygen atoms which are linked to the tetrahedral primary groups of the mordenite structure. The third peak at 1072.3-1072.5 eV in the Na 1s region corresponds to the sodium located in the zeolite framework.

Extended X-ray absorption fine structure (EXAFS)

EXAFS measurements are suitable to observe the local structure around the Ag^+ ions or Ag atoms attached to the zeolite framework. Thus, in order to shed more light into the oxidation state of silver in the Na-mordenite structure, *ex-situ* X-ray absorption spectroscopy studies were performed. The data obtained from the EXAFS spectra are shown in Table 2, while Figure 3 shows the Fourier transforms for the $Ag_{10}M$ (a) and $Ag_{15}M$ (b) samples. The k-range for the curve-fitting method was around 2.5-11.0 $Å^{-1}$.

The results in the Ag K-edge EXAFS show the presence of two coordination spheres of oxygen atoms around the Ag atoms. The results are similar in both samples. A coordination sphere with an average coordination number close to 1 and a second coordination sphere at a greater distance with a coordination number close to 2 are observed for the $Ag_{10}M$ and $Ag_{15}M$ samples. Each coordination sphere would probably correspond to different silver species bound to oxygen atoms. The Ag-O distance for the first fitted shell is similar to that found in Ag_2O,[41] while the second is compatible with Ag-O distances reported for Ag^+ exchanged in zeolites.[42] Thus, two Ag species would be present in both catalysts, a small proportion of Ag oxide, and another one with a greater Ag-O bond distance, which would correspond to Ag exchanged in the zeolite structure.

The most noticeable difference is observed in the average coordination number of the first coordination sphere which is somewhat higher for the $Ag_{15}M$ sample. This could indicate that a higher fraction of oxide is present in this sample or that the oxide clusters are slightly larger than those in $Ag_{10}M$. The TPR results[26, 27] shows that a higher silver content increases the amount of oxide formed in the sample volume.

X-ray absorption near edge spectroscopy (XANES)

An important advantage of this technique is that it is element specific, thus providing selective information on silver. Figure 4 shows the normalized L_3–edge XANES spectra of the silver obtained for two model compounds, Ag(0) and Ag_2O and for the $Ag_{15}M$ and $Ag_{10}M$ samples.

There is a clear difference between the spectra of the Ag-exchanged mordenite samples and the oxide, indicating that only a small fraction of Ag could be present as Ag_2O and different Ag species should be present in the samples, in agreement with EXAFS results.

The most remarkable feature of the spectrum is the peak at 3350 eV. This peak corresponds to a permitted transition $2p_{3/2} \rightarrow 4d$. Its intensity is directly related to the evacuation of Ag 4d states and it is higher in compounds with covalent bonds such as the Ag_2O oxide. The intensity observed for the $Ag_{15}M$ and $Ag_{10}M$ samples is lower than that observed for the oxide, and the peak is shifted to a lower energy, which indicates that Ag is mainly found in compounds with ionic character links with a longer Ag-O bond distance.[43]

In effect, the presence of this peak has already been assigned to Ag^+ ions exchanged to the cation-exchange sites of a zeolite.[44]

Figure 4 shows the spectra of the samples in the region of this peak. The peak for $Ag_{10}M$ is more intense than for the $Ag_{15}M$ sample. This would indicate that a higher proportion of silver is as Ag^+ exchanged in the zeolite in $Ag_{10}M$ sample, while a higher proportion of Ag_2O is present in the $Ag_{15}M$ sample.

UV-VIS DRS

The co-existence of different kinds of silver species can be discriminated by UV-Vis DRS. Figure 5 shows the UV-Vis DRS spectra of the calcined Ag_xM. The spectra of the

exchanged samples exhibit an intense UV absorption band at around 220 nm (the peak position of the band may exist in the wavelength region lower than 200 nm) which was attributed to $4d^{10} \rightarrow 4d^9 5s^1$ electron transition of isolated Ag^+ ions exchanged in the Na-mordenite matrix.[20, 45, 46] The spectrum for the Na-mordenite support showed no significant absorption bands.

The UV-Vis DRS absorption spectra in the region 220 – 400 nm were analyzed to understand the interaction of silver with the Na-mordenite structure. As shown in Figure 5, all the calcined Ag_xM samples also present bands at 270, 292 and 324 nm. These DRS bands are assigned to small silver cationic clusters $Ag_n^{\delta+}$ ($n < 10$) in agreement with those reported by other authors. Shibata et al.[47] observed bands assigned to the $Ag_n^{\delta+}$ clusters (260, 285 and 316 nm) in Ag-MFI after the C_3H_8-SCR in the presence of 0.2-0.5 % H_2. In addition, Figure 5 shows a broad band centered at 413 nm detected for all the Ag_xM solids. This band could be due to Ag_2O particles, which display capability of light absorption in both UV and visible range of 200-650 nm.[48] Gurin et al.[49, 50] linked the broadening in this region to oxide particles which have wide size distribution. Because of their size, that exceeds diameters of regular mordenite channels, these particles may be located at the outer surface of microcrystals or at the specific sites inside the mordenite matrix like cleaved areas or defects.

Therefore, the UV-Vis DRS spectra unambiguously demonstrate that Ag^+ ions, cationic clusters and Ag_2O particles are present in the calcined samples. These results are in agreement with those obtained by EXAFS, XANES and XPS techniques.

UV-Vis DRS spectra of $Ag_{15}M$ and $Ag_{10}M$ samples after using in SCR-NOx (spectra b) and adsorption/desorption of toluene (spectra c) are presented in Figure 6. These spectra are compared with the corresponding calcined samples (spectra a). Both $Ag_{15}M$ and $Ag_{10}M$ samples used in the chemical reaction (spectra b) present essentially the same

bands that in calcined samples (spectra a). The stability observed in the distribution of silver species could be associated with the good performance exhibited by the catalyst under reaction conditions.[26]

However, both spectra change after being used in the successive cycles of adsorption/desorption of toluene (Figure 6, spectra c). A decrease of the bands at low wavelengths (below 370 nm) is observed, corresponding to the decline of the isolated Ag^{+} ions and cationic clusters $Ag_n^{\delta+}$. Spectrum 'c' exhibits a widening and an increase of the intensity of the band above 350 nm. This broad band could be split in two signals. One at 410-415 nm corresponding to small particles of Ag_2O dispersed in the zeolitic matrix and another at 370-380 nm. A similar band was reported by several authors for Ag-zeolite after a reduction treatment in H_2 flow at 100 and 300 °C. This absorption band is assigned to ultrafine silver and associated with the Plasmon resonance in silver particles.[49, 51]

During the toluene desorption to 500 °C on the $Ag_{10}M$ and $Ag_{15}M$ samples, the formation of metallic silver particles was observed. In agreement with the results observed during temperature-programmed desorption of adsorbed toluene, above 250 °C products of the decomposition of toluene (such as H_2, CO_2 and water) were observed by mass spectroscopy of gaseous products. Thus, the produced hydrogen reduces the cationic clusters and Ag_xO particles to metallic silver.

Sitting and distribution of Ag species in mordenite

Through XPS, EXAFS/XANES and UV-Vis DRS it was determined that all the calcined samples exhibit Ag_2O particles dispersed in the mordenite. Besides, isolated Ag^{+} ions and $Ag_n^{\delta+}$ cationic clusters exchanged in different sites were observed. It is known that the metal ions can be located in a site called 'alpha' which corresponds to

the main channel of NaMOR, so that the oxygen atoms are coordinated to the 6-membered ring formed by two pentasil rings. These ions have the weaker bond with the oxygen of the zeolite structure. In contrast, the exchange sites known as 'beta' cavities are characterized as less accessible because they have relatively stronger bonds between the cation and the oxygen atoms of the zeolite structure as compared to the alpha site. At this site, the metal ions are coordinated with oxygens 8-membered ring of the cavity of the mordenite. The 'gamma' cationic site exchange provides high coordination with high bond strength between the cation and the oxygen atoms of the zeolite.[52, 53]

It is important to note that the population of individual sites with cations strongly depends on the concentration of Ag in the mordenite and the presence of co-cations.[54] Previous work of our group[26, 27] reported that Ag^+ ions are preferentially exchanged in the main channel (α/Ag^+) of the Na-mordenite structure, which can be reduced at moderate temperatures. A smaller fraction is sitting at more stable sites (side-pocket) where Ag^+ ions strongly interact with the atoms of the structure (β/Ag^+).

Role of silver species on the catalytic behavior

The silver species present in the Ag_xM catalysts are the active centers for the selective catalytic reduction of NOx with butane as the reducing agent in the presence of oxygen excess. In this sense, the complex reaction system can be visualized as the competition between NO and O_2 for a limited amount of hydrocarbon and for the number of active sites. Basically, two main reactions occur simultaneously, one the reduction of NOx to N_2 and the hydrocarbon combustion. It is important to study the catalytic behavior simulating reaction conditions close to the real, ie. higher space velocities, oxidizing atmosphere and presence of water vapor.

In this sense, with all the spectroscopic evidence obtained the following model could be proposed to depict the role of silver species in the SCR-NOx with butane (Figure 7).

In agreement with other authors[55-57] is recognized that silver oxides and silver cations in zeolites are active centers for the SCR of NOx. Furthermore, the mordenite structure, with a system of parallel channels and high surface area, promotes a good distribution of these centers. In this vein, the butane and the NOx reactants could be adsorbed over the silver ions exchanged in more accessible sites inside the mordenite to produces carbon dioxide, water and nitrogen (Figure 7, R1).

Simultaneously, the reaction between NO and Ag_2O, produces NO_2 and Ag(0) through a redox process (Fig. 7, R2). A side reaction, the butane oxidation on the silver oxide and Ag^+ cations, produces carbon dioxide and water (Fig. 7, R3).

Role of silver species on the adsorption/desorption process

In our previous results,[26] the Ag_xM samples showed a good adsorption capacity of toluene at 100 °C which it was increased with the metal content. During the adsorption process at low temperature, the toluene shows a strong interaction with Ag^+ ions exchanged in mordenite sites (α, β, δ) through the aromatic ring. In addition, during the desorption process (300-500 °C), hydrogen, carbon dioxide and water were observed as products of toluene decomposition. As the temperature increases, the reaction of toluene with cationic clusters and silver oxide is favored (Figure 8, R1 and R2). In addition, they can be reduced by the presence of hydrogen (Figure 8, R3).

In this case, unlike the behavior in the SCR-NOx, the presence of silver oxide particles has the advantage of providing Ag^+ sites for adsorption and retention to higher temperatures. However, it also promotes the partial oxidation of toluene at higher temperatures.

Conclusions

Na-mordenite zeolite with 5, 10 and 15 wt. % of Ag was characterized by spectroscopic techniques. Different types of silver species were found in these catalysts, depending on the type of treatment or reaction conditions under which the sample was studied. In the samples prepared by silver ion exchange and calcined in O_2 flow at 500 °C, isolated Ag^+ cations, cationic clusters $Ag_n^{\delta+}$ ($n < 10$) and Ag_xO particles coexisted. These species were identified by the UV-Vis Diffusive Reflectance, where the absorption spectra showed an intense UV absorption band at around 220 nm (Ag^+), bands at 270, 292 and 324 nm ($Ag_n^{\delta+}$) and a weak band around 400–500 nm (Ag_xO). EXAFS and XANES studies confirmed the presence of silver oxides and cationic silver species. In addition, through the modified Auger parameter (α'), calculated from XPS measurements, it was possible to identify Ag^+ ions at exchange sites (α'~722 eV) and Ag_xO (α'~725 eV) highly dispersed on the surface. Both species constitute stable active centers for the SCR of NOx under severe reaction conditions. However, during the adsorption-desorption of toluene, the reduction of silver oxides produces Ag(0) due to thermal hydrocarbon decomposition.

Acknowledgements

This work was supported by LNLS, Brazil (Project SXS-10877), ANPCyT (PICT-2008-00038) and CONICET (PIP 112-200801-03079). The authors also acknowledge the financial support received from UNL and CONICET. They are grateful to ANPCyT for the purchase of the SPECS multitechnique analysis instrument (PME8-2003) and the UV-Vis spectrometer (PME 311). Thanks are given to Fernanda Mori for the XPS measurements and to Elsa Grimaldi for the English language editing.

References

(1) Waterhouse, G. I. N.; Bowmaker, G. A.; Metson, J. B. Oxidation of Polycrystalline Silver Foil by Reaction With Ozone. *Appl. Surf. Sc.* **2001**, *183*, 191-204.

(2) Gao, X-Y.; Wang, S-Y.; Li, J.; Zheng, Y-X.; Zhang, R-J.; Zhou, P.; Yang, Y-M.; Chen, L-Y. Study of Structure and Optical Properties of Silver Oxide Films by Ellipsometry, XRD, and XPS Methods. *Thin Sol. Films* **2004**, *455-456*, 438-442.

(3) Ju, W-S.; Matsuoka, M.; Iino, K.; Yamashita, H.; Anpo, M. The Local Structures of Silver (I) Ion Catalysts Anchored Within Zeolite Cavities and Their Photocatalytic Reactivities for the Elimination of N_2O into N_2 and O_2. *J. Phys. Chem. B* **2004**, *108*, 2128-2133.

(4) Bera, S.; Gangopadhyay, P.; Nair, K. G. M.; Panigrahi, B. K.; Narasimhan, S. V. Electron Spectroscopy Analysis of Silver Nanoparticles in a Soda-Glass. *J. Elect. Spectr. Rel. Phen.* **2006**, *152*, 91-95.

(5) Ausavasukhi, A.; Suwannaran, S.; Limtrakul, J.; Sooknoi, T. Reversible Interconversion Behavior of Ag Species in AgHZSM-5: XRD, ^{1}H MAS NMR, TPR, TPHE, and Catalytic Studies. *Appl. Catal. A: Gen.* **2008**, *345*, 89-95.

(6) Kaspar, T. C.; Droubay, T.; Chambers, S. A.; Bagus, P. S. Spectroscopic Evidence for Ag(III) in Highly Oxidized Silver Films by X-Ray Photoelectron Spectroscopy. *J. Phys. Chem. C* **2010**, *114*, 21562-21571.

(7) Waterhouse, G. I. N.; Metson, J. B.; Bowmaker, G. A. Synthesis, Vibrational Spectra and Thermal Stability of Ag_3O_4 and Related Ag_7O_8X Salts ($X=NO_3^-$, ClO_4^-, HSO_4^-). *Polyhedron* **2007**, *26*, 3310-3322.

(8) Naydenov, A.; Konova, P.; Nikolov, P.; Klingstedt, F.; Kumar, N.; Kovacheva, D.; Stefanov, P.; Stoyanova, R.; Mehandjiev, D. Decomposition of Ozone on Ag/SiO_2 Catalyst for Abatement of Waste Gases Emissions. *Catal. Today* **2008**, *137*, 471-474.

(9) Shimizu, K.; Shibata, J.; Yoshida, H.; Satsuma, A.; Hattori, T. Silver-Alumina Catalysts for Selective Reduction of NO by Higher Hydrocarbons: Structure of Active Sites and Reaction Mechanism. *Appl. Catal B: Env.* **2001**, *30*, 151-162.

(10) Iglesias-Juez, A.; Hungría, A. B.; Martínez-Arias, A.; Fuerte, A.; Fernandez-García, M.; Anderson, J. A.; Conesa, J. C.; Soria, J. Nature and Catalytic Role of Active Silver Species in the Lean NOx Reduction With C_3H_6 in the Presence of Water. *J. Catal.* **2003**, *217*, 310-323.

(11) Iliopoulou, E. F.; Evdou, A. P.; Lemonidou, A. A.; Vasalos, I. A. Ag/Alumina Catalysts for the Selective Catalytic Reduction of NOx and Using Various Reductants. *Appl. Catal. A: Gen.* **2004**, *274*, 179-189.

(12) Breen, J. P.; Burch, R.; Hardacre, C.; Hill, C. J.; Krutzsch, B.; Bandl-Konrad, B.; Jobson, E.; Cider, L.; Blakeman, P. G.; Peace, L. J.; Twigg, M. V.; Preis, M.; Gottschling, M. An Investigation of the Thermal Stability and Sulphur Tolerance of $Ag/\gamma\text{-}Al_2O_3$ Catalysts for the SCR of NOx with Hydrocarbons and Hydrogen. *Appl. Catal. B: Env.* **2007**, *70*, 36-44.

(13) Kannisto, H.; Ingelsten, H. H.; Skoglundh, M. Ag/Al_2O_3 Catalysts for Lean NOx Reduction – Influence of Preparation Method and Reductant. *J. Mol. Catal. A: Chem.* **2009**, *302* 86-96.

(14) Sitshebo, S.; Tsolakis, A.; Theinnoi, K.; Rodríguez-Fernández, J.; Leung, P. Improving the Low Temperature NOx Reduction Activity Over a $Ag\text{-}Al_2O_3$. *Chem. Eng. J.* **2010**, *158*, 402-410.

(15) Sawatmongkhon, B.; Tsolakis, A.; Sitshebo, S.; Rodríguez-Fernández, J.; Ahmadinejad, M.; Collier, J.; Rajaram, R. R. Understanding the Ag/Al_2O_3 Hydrocarbon-SCR Catalyst Deactivation Through TG/DT Analysis of Different Configurations. *Appl. Catal. B: Env.* **2010**, *97*, 373-380.

(16) Demidyuk, V.; Hardacre, C.; Burch, R.; Mhadeshwar, A.; Norton, D.; Hancu, D. Aromatic Hydrocarbons and Sulfur Based Catalyst Deactivation for Selective Catalytic Reduction of NOx. *Catal. Today* **2011**, *164*, 515-519.

(17) Rao, K. N.; Ha, H. P. SO_2 Promoted Alkali Metal Doped Ag/Al_2O_3 Catalysts for CH_4-SCR of NOx. *Appl. Catal. A: Gen.* **2012**, *433-434*, 162-169.

(18) Sebastian, J.; Jasra, R. V. Sorption of Nitrogen, Oxygen, and Argon in Silver-Exchanged Zeolites. *Ind. Eng. Chem. Res.* **2005**, *44*, 8014-8024.

(19) Ferreira, L.; Fonseca, A. M.; Botelho, G.; Almeida-Aguilar, C.; Neves, I. C. Antimicrobial Activity of Faujasite Zeolites Doped With Silver. *Microp. Mesop. Mater.* **2012**, *160*, 126-132.

(20) Shi, C.; Cheng, M.; Qu, Z.; Bao, X. Investigation on the Catalytic Roles of Silver Species in the Selective Catalytic Reduction of NOx With Methane. *Appl. Catal. B: Env.* **2004**, *51*, 171-181.

(21) Shibata, J.; Shimizu, K.; Takada, Y.; Shichi, A.; Yoshida, H.; Satokawa, S.; Satsuma, A.; Hattori, T. Structure of Active Ag Clusters in Ag Zeolites for SCR of NO by Propane in the Presence of Hydrogen. *J. Catal.* **2004**, *227*, 367-374.

(22) Shi, C.; Cheng, M.; Qu, Z.; Bao, X. On the Correlation Between Microstructural Changes of Ag-H-ZSM-5 Catalysts and Their Catalytic Performances in the Selective Catalytic Reduction of NOx by Methane. *J. Mol. Catal. A: Chem.* **2005**, *235*, 35-43.

(23) Masuda, K.; Tsujimura, K.; Shinoda, K.; Kato, T. Silver-Promoted Catalyst for Removal of Nitrogen Oxides From Emission of Diesel Engines. *Appl. Catal. B: Env.* **1996**, *8*, 33-40.

(24) Bartolomeu, R.; Henriques, C.; da Costa, P.; Ribeiro, F. deNOx over Ag/H-ZSM-5: Study of NO_2 Interaction With Ethanol. *Catal. Today* **2011**, *176*, 81-87.

(25) Männikkö, M.; Skoglundh, M.; Ingelsten, H. H. Selective Catalytic Reduction of NOx With Methanol over Supported Silver Catalysts. *Appl. Catal. B: Env.* **2012**, *119-120*, 256-266.

(26) Aspromonte, S. G.; Serra, R. M.; Miró, E. E.; Boix, A. V. AgNaMordenite Catalysts for Hydrocarbon Adsorption and deNOx Process. *Appl. Catal. A: Gen.* **2011**, *407*, 134-144.

(27) Aspromonte, S.; Miró, E.; Boix, A. FTIR Studies of Butane, Toluene and Nitric Oxide Adsorption on Ag Exchanged NaMordenite. *Adsorption* **2012**, *18*, 1-12.

(28) Briggs, D.; Seah, M. P. *Practical Surface Analysis, second ed.*; John Wiley & Sons, New York, **1992**.

(29) Ankudinov, A. L.; Ravel, B.; Rehr, J. J.; Conradson, S. D. Real-Space Multiple Scattering Calculation and Interpretation on X-Ray-Absorption Near-Edge Structure. *Phys. Rev. B* **1998**, *58*, 7565-7576.

(30) Ravel, B.; Newville, M. ATHENA, ARTEMIS, HEPHAESTUS: Data Analysis for X-Xay Absorption Spectroscopy Using IFEFFIT. *J. Synch. Rad.* **2005**, *12*, 537-541.

(31) Abbate, M.; Vicentin, F. C.; Compagnon-Cailhol, V.; Rocha, M. C.; Tolentino, H. The Soft X-Ray Spectroscopy Beamline at the LNLS: Technical Description and Commissioning Results. *J. Synch. Rad.* **1999**, *6*, 964-972.

(32) Fonseca, A. M.; Neves, I. C. Study of Silver Species Stabilized in Different Microporous Zeolites. *Microp. Mesop. Mater.* **2013**, *181*, 83-87.

(33) Ju, W-S.; Matsuoka, M.; Iino, K.; Yamashita, H.; Anpo, M. The Local Structures of Silver (I) Ion Catalysts Anchored Within Zeolite Cavities and Their Photocatalytic Reactivities for the Elimination of N_2O into N_2 and O_2. *J. Phys. Chem. B* **2004**, *108*, 2128-2133.

(34) Shen, J.; Shan, W.; Zhang, Y.; Du, J.; Xu, H.; Fan, K.; Shen, W.; Tang, Y. Gas-Phase Selective Oxidation of Alcohols: In Situ Electrolytic Nano-Silver/Zeolite Film/Copper Grid Catalyst. *J. Catal.* **2006,** *237*, 94-101.

(35) Miao, S.; Wang, Y.; Ma, D.; Zhou, S.; Su, L.; Tan, D.; Bao, X. Effect of Ag^+ Cations on Monoxidative Activation of Methane to C_2-Hydrocarbons. *J. Phys. Chem. B* **2004,** *108*, 17866-17871.

(36) Kim, Y. H.; Lee, D. K.; Cha, H. G.; Kim, C. W.; Kang, Y. S. Synthesis and Characterization of Antibacterial Ag-SiO_2 Nanocomposite. *J. Phys. Chem. C* **2007,** *111*, 3629-3635.

(37) Weaver, J. F.; Hoflund, G. B. Surface Characterization Study of the Thermal Decomposition of AgO. *J. Phys. Chem.* **1994**, *98*, 8519-8524.

(38) NIST database Webbook Chemistry, available http://webbook.nist.gov/chemistry.

(39) Bassett, P. J.; Gallon, T. E.; Matthew, J. A. D.; Prutton, M. Quasi-Atomic Fine Structure in the Auger Spectra of Solid Silver and Indium. *Surf. Sci.* **1973**, *35*, 63-74.

(40) Ferraria, A. M.; Carapeto, A. P.; Botelho do Rego, A. M. X-Ray Photoelectron Spectroscopy: Silver Salts Revisited. *Vacuum* **2000,** *86*, 1988-1991.

(41) Norby, P.; Dinnebier, R.; Fitch, A. N. Decomposition of Silver Carbonate; the Crystal Structure of Two High Temperature. *Inorg. Chem.* **2002,** *41,* 3628-3637.

(42) Bordiga, S.; Turnes Palomino, G.; Arduino, D.; Lamberti, C.; Zecchina, A.; Otero, Areán, C. Well-Defined Carbonyl Complexes in Ag^+- and Cu^+- Exchanged ZSM-5 Zeolite: a Comparison With Homogeneous Counterparts. *J. Mol. Catal. A* **1999,** *146*, 97-106.

(43) Natoli C. R. Distance Dependence of Continuum and Bound State of Excitonic Resonances in X-Ray Absorption Near Edge Structures (XANES). EXAFS and Near Edge Structure III*,* Springer Proc. Phys. 2, **1984.**

(44) Shimizu, K.; Kobayashi, N.; Satsuma, A.; Kojima, T.; Satokawa, S. Mechanistic Study on Adsorptive Removal of Tert-Butanethiol on Ag-Y Zeolite Under Ambient Conditions. *J. Phys. Chem. B* **2006,** *110*, 22570-22576.

(45) Li, Z.; Flytzani-Stephanopoulos, M. On the Promotion of Ag-ZSM-5 by Cerium for the SCR of NO by Methane *J. Catal.* **1999**, *182*, 313-327.

(46) Keshavaraja, A.; She, X.; Flytzani-Stephanopoulos, M. Selective Catalytic Reduction of NO With Methane over Ag-Alumina Catalysts. *Appl. Catal. B: Env.* **2000**, *27*, L1-L9.

(47) Shibata, J.; Takada, Y.; Shichi, A.; Satokawa, S.; Satsuma, A.; Hattori, T. Ag Cluster as Active Species for SCR of NO by Propane in the Presence of Hydrogen over Ag-MFI. *J. Catal.* **2004**, *222*, 368–376.

(48) Zhou, W.; Liu, H.; Wang, J.; Liu, D.; Du, G.; Cui, J. Ag_2O/TiO_2 Nanobelts Heterostructure With Enhanced Ultraviolet and Visible Photocatalytic Activity. *Appl. Mater. Interf.* **2010**, *2* 2385–2392.

(49) Gurin, V. S.; Bogdanchikova, N. E.; Petranovskii, V. P. Self-Assembling of Silver and Copper Small Clusters Within the Zeolite Cavities: Prediction of Geometry. *Mat. Sc. Eng. C* **2001**, *18,* 37-44.

(50) Gurin, V. S.; Petranovskii, V. P.; Hernandez, M. A.; Bogdanchikova, N. E.; Alexeenko, A. A. Silver and Copper Clusters and Small Particles Stabilized Within Nanoporous Silicate-Based Materials. *Mat. Sc. Eng. A* **2005**, *391*, 71-76.

(51) Yin, A.; Wen, C.; Dai, W-L.; Fan, K. Ag/MCM41 as a Highly Efficient Mesostructured Catalyst for the Chemoselective Synthesis of Methyl Glycolate and Ethyleneglycol. *Appl. Catal. B: Env.* **2011**, *108-109*, 90-99.

(52) Kaucky, D.; Vondrová, A.; Dedecek, J.; Wichterlová, B. Activity of Co Ion Sites in ZSM-5, Ferrierite, and Mordenite in Selective Catalytic Reduction of NO With Methane. *J. Catal.* **2000,** *194*, 318-329.

(53) Cejka, J.; Kapustin, G. A.; Wichterlová, B. Factors Controlling Iso-/n- and Para-Selectivity in the Alkylation of Toluene With Isopropanol on Molecular Sieves. *Appl. Catal.A: Gen.* **1994,** *108*, 187-204.

(54) Dedecek, J.; Wichterlová, B. Co^{2+} Ion Sitting in Pentasil-Containing Zeolites. I. Co^{2+} Ion Sites and Their Occupation in Mordenite. A Vis NIR Diffuse Reflectance Spectroscopy Study. *J. Phys. Chem. B* **1999,** *103*, 1462-1476.

(55) Tamm, S.; Ingelsten, H. H.; Palmqvist, A. E. C. On the Different Roles of Isocyanate and Cyanide Species in Propene-SCR over Silver/Alumina. *J. Catal.* **2008,** *255*, 304-312.

(56) Mhadeshwar, A. B.;Winkler, B. H.; Eiteneer, B.; Hancu, D. Microkinetic Modelling for Hydrocarbon (HC)-Based Selective Catalytic Reduction (SCR) of NOx on a Silver-Based Catalyst. *Appl. Catal. B: Env.* **2009,** *89*, 229-238.

(57) Flura, A.; Can, F.; Courtois, X.; Royer, S.; Duprez, D. High-Surface-Area Zinc Aluminate Supported Silver Catalysts for Low Temperature SCR of NO With Ethanol. *Appl. Catal. B: Env.* **2012,** *126*, 275-289.

Table of contents (TOC) Image

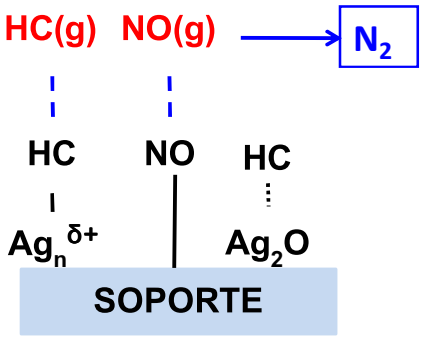

Tables.

Table 1. Results obtained from XPS measurements.

Samples	Treatment[1]	BE Ag $3d_{5/2}$ (fwhm) eV [2]	α' (eV) [3]	Ag/Al
$Ag_{15}M$	a	368.5 (2.4)	721.8	1.2
	b	367.6 (2.0)	726.3	0.3
	c	368.6 (2.0)	720.8	1.2
	d	368.4 (2.4)	721.9	0.7
$Ag_{10}M$	a	368.6 (2.1)	722.1	1.0
	b	367.5 (2.0)	726.3	0.3
	c	368.6 (2.2)	721.9	0.9
	d	368.1 (2.6)	721.5	0.8
Ag_5M	a	368.6 (2.1)	721.8	0.7
	b	368.6 (2.1)	726.8	0.7
Ag_2O/M	e	367.8 (1.9)	724.9	0.3
	b	367.0 (1.6)	726.4	0.3
Ag(0) foil	f	368.4 (1.5)	726.2	-
Ag_2O pure	g	368.2 (1.8)	723.4	-
	b	368.4 (1.8)	726.9	-
$AgNO_3$	h	368.2 (2.0)	723.4	-

(1) Treatments: (a) calcined in O_2 flow at 500 °C, (b) reduced *in situ* with H_2 (5 %)/Ar flow at 400 °C for 10 min, (c) used in the SCR-NOx with butane, NO, O_2 and 2 % H_2O, (d) used as adsorbent in three cycles of toluene adsorption/desorption, (e) evacuated at 300 °C during 30 min, (f) Cleaned the surface by argon ion sputtering, (h) without treatment before the measure.
(2) Binding energy and the full width at half maximum (eV).
(3) Modified Auger parameter: α' (eV) = KE (Ag M_4NN) – KE (Ag $3d_{5/2}$) + 1253.6 eV.

Table 2. Results obtained from Ag K-edge EXAFS analysis.

Sample	Neighbor	N (1)	R (2)	σ^2 (3)
$Ag_{10}M$	O	0.9 ± 0.2	2.08 ± 0.07	0.004 ± 0.001
		2.3 ± 0.3	2.32 ± 0.08	0.004 ± 0.001
$Ag_{15}M$	O	1.3 ± 0.2	2.01 ± 0.06	0.004 ± 0.001
		2.1 ± 0.3	2.28 ± 0.08	0.005 ± 0.001

(1) Average Coordination Number.

(2) Interatomic Distance (Å).

(3) Debye-Waller factor ($Å^2$).

Figure Captions

Figure 1. XPS data of $Ag_{15}M$ (A, B) and pure compounds (C, D). Treatments: (a) calcined in O_2 flow at 500 °C, (b) reduced in H_2 flow at 400 °C, (c) used in SCR-NOx reaction, (d) used in adsorption-desorption of toluene. Pure compounds: (e) $AgNO_3$, (f) Ag_2O, (g) Ag_2O *in situ* reduced at 300 ºC and (h) Ag(0) foil. Small vertical lines indicates the peaks used to calculating the modified Auger parameter.

Figure 2. (A) Ag 3d core-level and (B) Ag MNN Auger transition spectra of $Ag_{10}M$ sample after different treatments: (a) calcined in O_2 flow at 500 °C, (b) reduced in H_2 flow at 400 °C, (c) used in SCR-NOx reaction and (d) used in adsorption-desorption of toluene. Small vertical lines indicates the peaks used to calculating the modified Auger parameter

Figure 3. Fourier Transforms of the EXAFS oscillation at the Ag K-edge (solid line) and their corresponding fits (dashed line) of (A) $Ag_{10}M$ and (B) $Ag_{15}M$ samples.

Figure 4. Normalized Ag L_3-edge XANES spectra.

Figure 5. UV-Vis DRS spectra of calcined Ag_xM catalysts.

Figure 6. UV-Vis DRS spectra of (A) $Ag_{15}M$ and (B) $Ag_{10}M$ samples; (a) calcined in air at 500 °C, (b) used under NOx-SCR with butane, 2 % O_2 and 2 % H_2O and (c) used in adsorption-desorption process of toluene/He.

Figure 7. Role of silver species in the reaction system of the SCR-NOx with butane.

Figure 8. Model of the behavior of silver species in the adsorption/desorption of toluene.

Figures.

Figure 1.

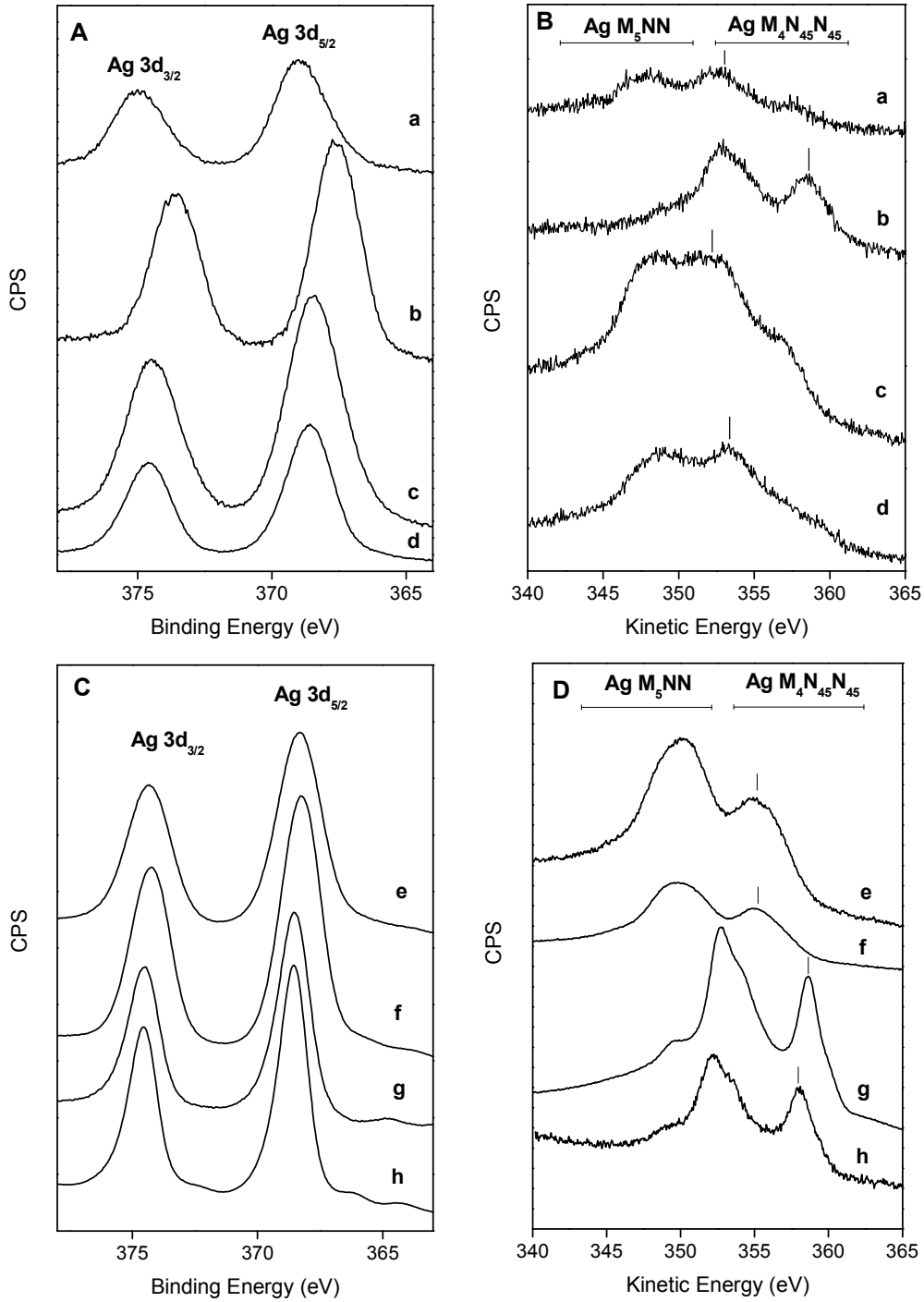

Figure 2.

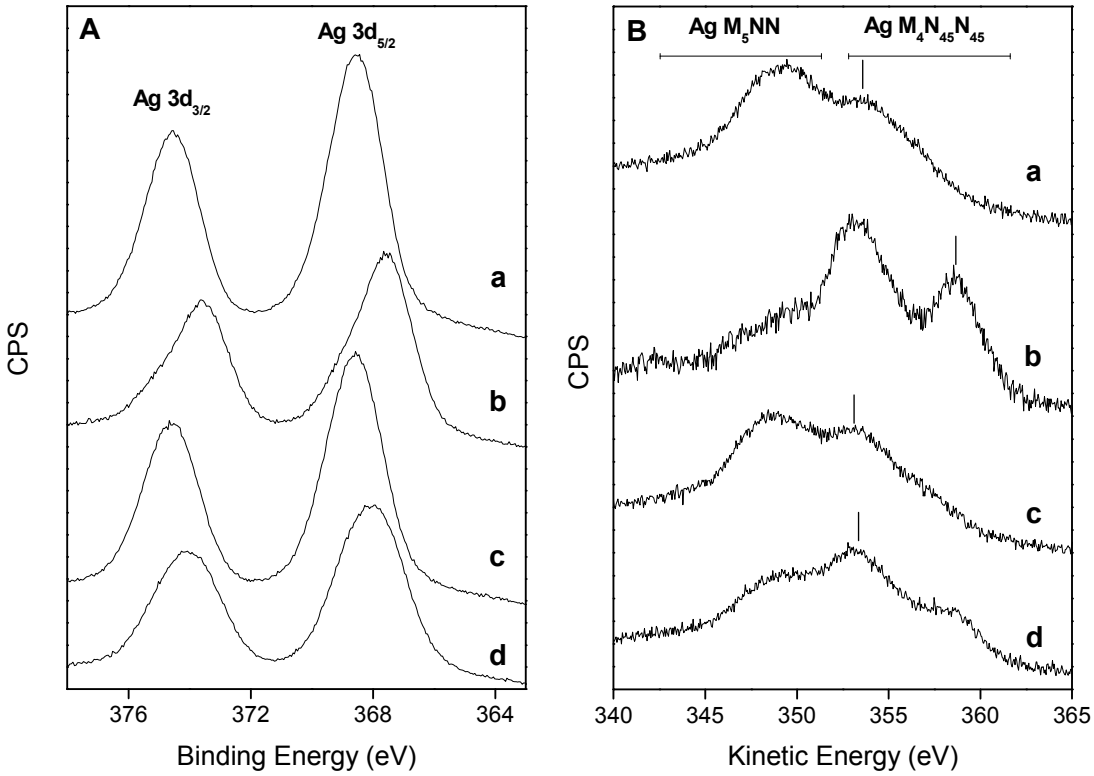
A
Ag 3d5/2
Ag 3d3/2
a
b
c
d
CPS
376
372
368
364
Binding Energy (eV)
B
Ag M5NN
Ag M4N45N45
a
b
c
d
CPS
340
345
350
355
360
365
Kinetic Energy (eV)

Figure 3.

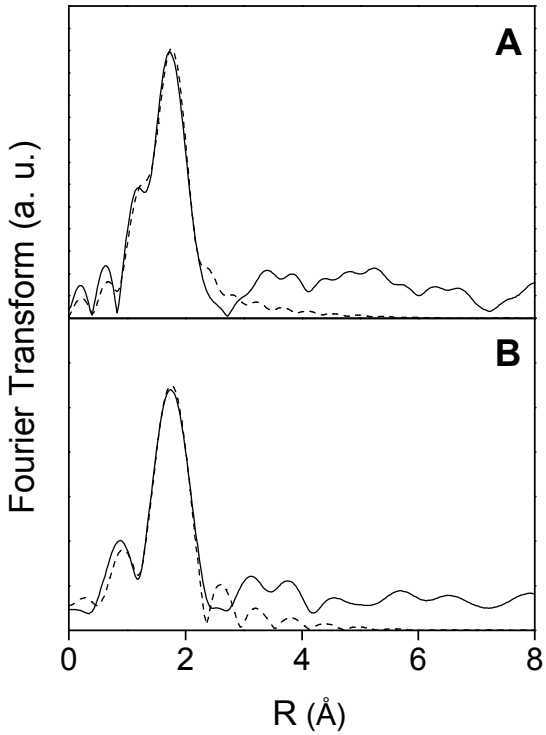

Figure 4.

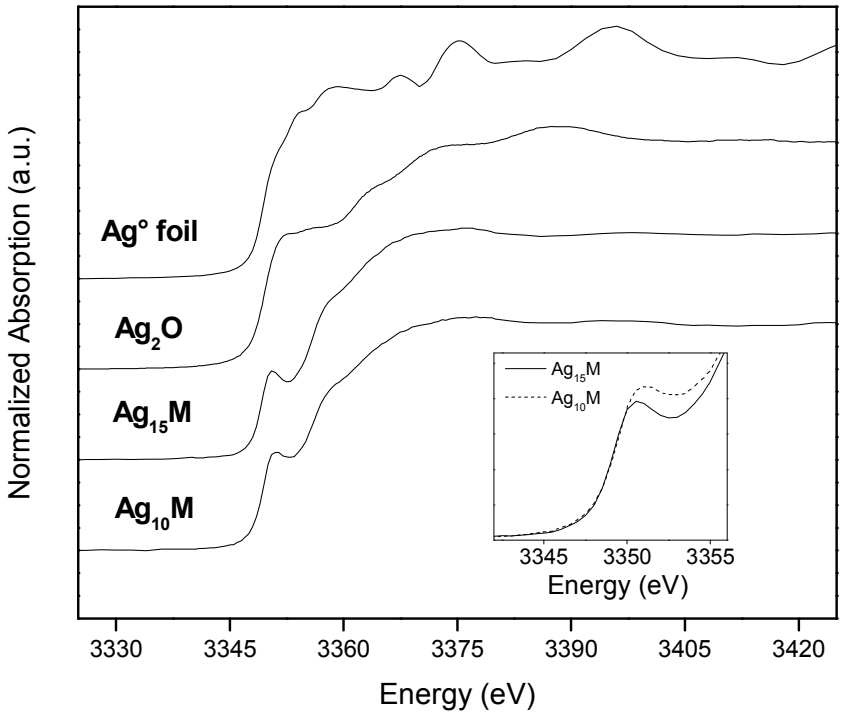
Normalized Absorption (a.u.)
Ag° foil
Ag2O
Ag15M
Ag10M
Ag15M
Ag10M
3345
3350
3355
Energy (eV)
3330
3345
3360
3375
3390
3405
3420
Energy (eV)

Figure 5.

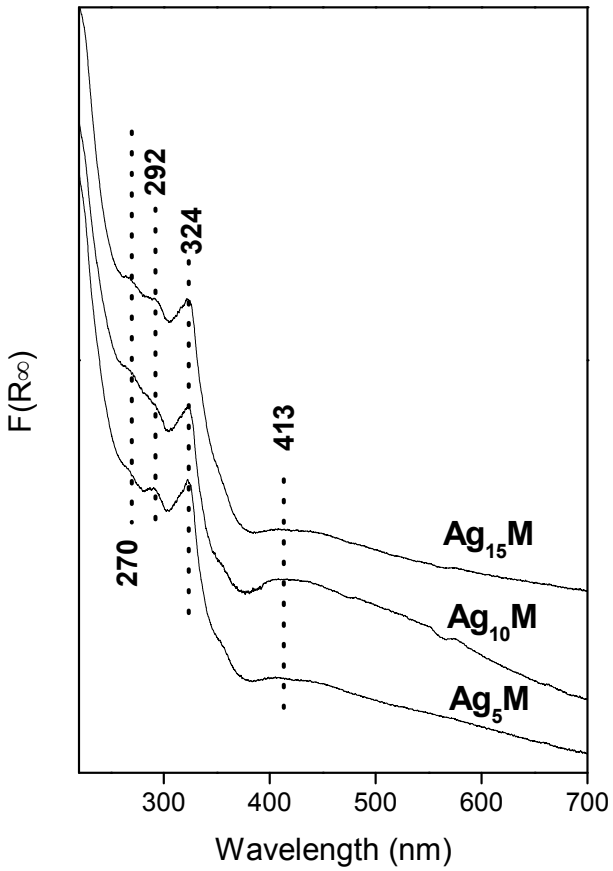
F(R∞)
292
324
413
270
Ag15M
Ag10M
Ag5M
300
400
500
600
700
Wavelength (nm)

Figure 6.

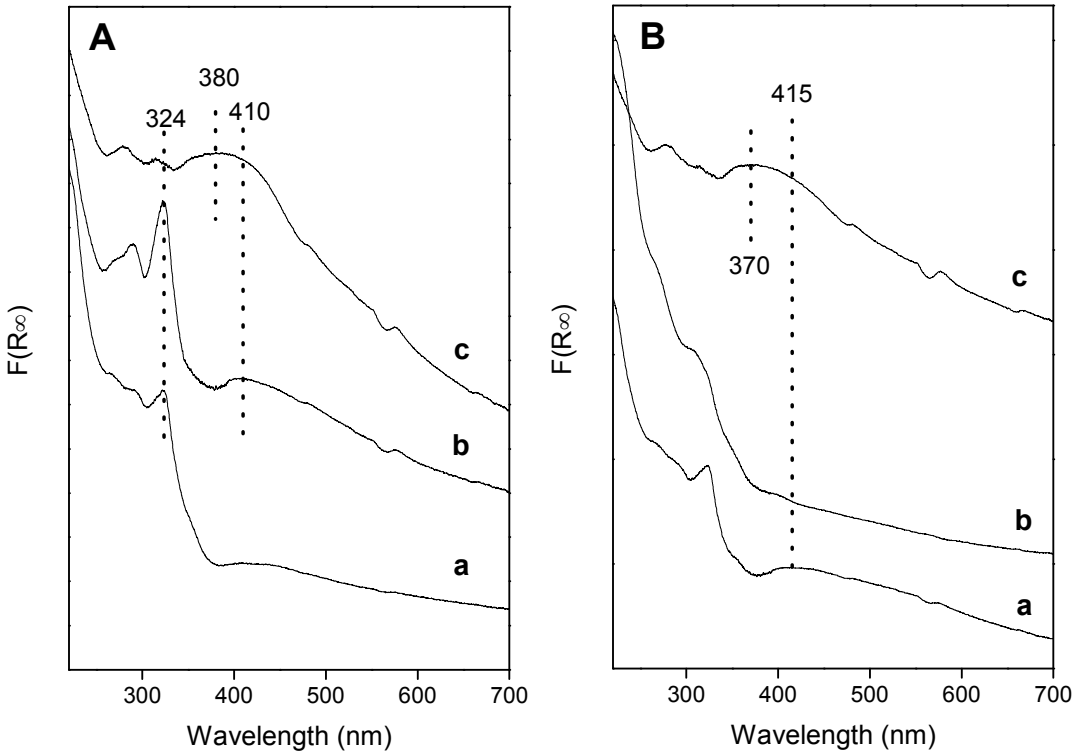
A
380
324
410
c
b
a
F(R∞)
300
400
500
600
700
Wavelength (nm)
B
415
370
c
b
a
F(R∞)
300
400
500
600
700
Wavelength (nm)

Figure 7.

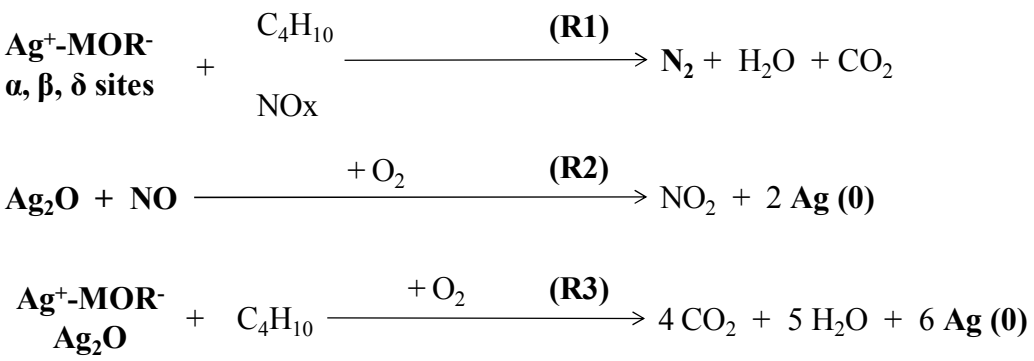
Ag+-MOR-
α, β, δ sites
+
C4H10
NOx
(R1)
N2 + H2O + CO2
Ag2O + NO
+ O2
(R2)
NO2 + 2 Ag (0)
Ag+-MOR-
Ag2O
+ C4H10
+ O2
(R3)
4 CO2 + 5 H2O + 6 Ag (0)

Figure 8.

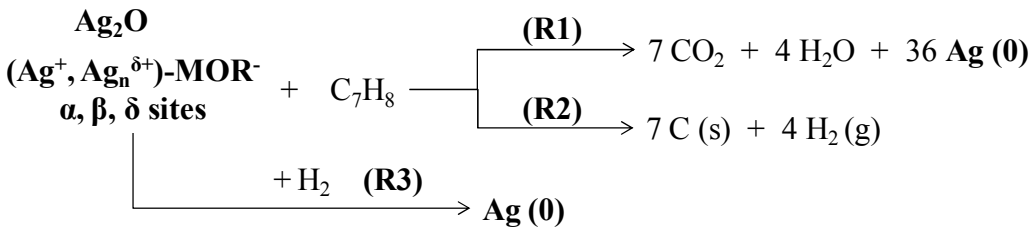
Ag2O
(Ag+, Agnδ+)-MOR-
α, β, δ sites
+ C7H8
(R1)
7 CO2 + 4 H2O + 36 Ag (0)
(R2)
7 C (s) + 4 H2 (g)
+ H2 (R3)
Ag (0)